Hindawi
Science and Technology of Nuclear Installations
Volume 2022, Article ID 2957310, 13 pages
https://doi.org/10.1155/2022/2957310

Research Article

Analysis of Heat Release Processes inside Storage Facilities Containing Irradiated Nuclear Graphite

Alexander O. Pavliuk,[1] **Evgeniy V. Bespala**,[2] **Sergey G. Kotlyarevskiy**,[1] **Ivan Yu. Novoselov**,[3] **and Veleriy N. Kotov**[2]

[1]*Pilot and Demonstration Center for Decommissioning of Uranium-Graphite Nuclear Reactors, Avtodoga 13 St., 179a, Seversk 636000, Russia*
[2]*Mining and Chemical Combine, Lenina St. 53, Zheleznogorsk 662972, Russia*
[3]*National Research Tomsk Polytechnic University, Lenin Ave. 30, Tomsk 634050, Russia*

Correspondence should be addressed to Alexander O. Pavliuk; pavliuk.grapa@yandex.ru

Received 1 August 2021; Revised 22 November 2021; Accepted 11 January 2022; Published 30 January 2022

Academic Editor: Klaudio Bari

The article is dedicated to the safety assessment of mixed storage of irradiated graphite and other types of radioactive waste accumulated during the operation of uranium-graphite reactors. The analysis of heat release processes inside storages containing irradiated nuclear graphite, representing a potential hazard due to the possible heating and, accordingly, the release of long-lived radionuclides during oxidation was carried out. The following factors were considered as the main factors that can lead to an increase in the temperature inside the storage facility: corrosion of metallic radioactive waste, the presence of fuel fragments, and also the random exposure of irradiated graphite to local sources of thermal energy (spark, etc.). It was noted in the work that the combined or separate influence of some factors can lead to an increase in the temperature of the onset of the initiation of Wigner energy release in graphite radwaste ($T_{in} \approx 90–100^{\circ}C$ for the "Worst-case" graphite). The model of heat generation in the storage was developed based on the analysis of the features of graphite radioactive waste storage and Wigner energy release. The layered location of different types of waste (graphite and aluminum) and the local character of the distribution of heat sources were adopted in this model. The greatest heating is achieved if graphite radioactive waste is located near the concrete walls of the storage facility, as well as in direct contact with irradiated aluminum radioactive waste, which was shown in this paper.

1. Introduction

Currently, more than 250,000 tons of graphite radioactive wastes have already been accumulated worldwide [1]. At the same time, approximately 60,000 tons of irradiated graphite was accumulated in the Russian Federation during the operation of various types of uranium-graphite reactors (UGR). To date, 13 production uranium-graphite reactors (PUGR), AM and AMB-100, AMB-200 Beloyarsk NPPs reactors, 1 RBMK reactor (the first power unit of the Leningrad NPP), and 1 EGP-6 reactor at the Bilibino NPP have been shut down. However, 9 RBMK reactors (Leningrad, Kursk, Smolensk NPPs) and 3 EGP-6 reactors are in operation [2].

Replaceable (temporary) structural elements, including graphite sleeves, thermal contact rings, displacers, fragmented aluminum channels, etc., were periodically removed during operation of the UGR. A part of the removed irradiated elements was placed in special containers. Another part of the mixed radioactive waste was sent to the reactor storage facilities of various types (depending on the type of UGR and the hydrogeological features of the site). It is worth noting that 25% of the total graphite has been accumulated as replaceable elements in Russia. ANDRA estimates that about 17% of the graphite was accumulated as graphite sleeves in France [3]. Situations with mixed storage of graphite and nongraphite radioactive wastes are also noted in Lithuania, the UK, and other countries [4, 5]. Elements from Magnox and aluminum alloys are also found with graphite in some radioactive waste storage facilities. There is a mixing of graphite with cement (cementing of graphite waste) or pouring them with cement.

At present, the demolition of these storages is difficult due to the lack of solutions to the problems of further handling of irradiated graphite and insufficient knowledge of safety issues during their dismantling [6]. The main issues related to ensuring safety before and after the dismantling of objects containing graphite include the necessity for annealing of graphite radioactive waste and the applicability of disposal methods, including grouting with a heated concrete composition [7].

An essential feature of graphite radioactive waste in storage facilities is the presence of stored energy (Wigner energy) in them [8, 9]. This is due to radiation damage to the crystal lattice of graphite and the accumulation of defects [10–12] when it is irradiated in UGR. In the Russian Federation, studies show that the maximum values of Wigner energy are recorded precisely in replaceable graphite elements. Moreover, the values significantly exceed the values obtained for graphite blocks [13].

The International Atomic Energy Agency (IAEA) organized the GRAPA project [14] aimed at pilot testing of solutions and technologies for the handling of irradiated graphite. One of the tasks of the GRAPA project is a detailed analysis of issues related to the effect of accumulation and release of stored energy in irradiated graphite, determination of emission parameters, and safety criteria. The parameters characterizing the accumulation and release of stored energy in graphite determine the conditions and possible consequences of its release (thermal effects) during the decommissioning of UGR. This also applies to work related to the handling of irradiated graphite, including the processing, storage, and disposal of graphite radioactive waste.

At the same time, a generalized analysis of the possibility of Wigner energy release for various options for handling irradiated graphite (in-situ entombment of UGR, aging, and dismantling of UGR, storage in containers of recycled or untreated graphite radioactive waste, etc.) showed that it is the mixed storage of graphite radioactive waste in storage facilities (belonging to the nuclear legacy) that causes the greatest trouble. Therefore, a detailed study of this issue, taking into account all the features of the storage of radioactive waste, is required.

2. Features of Storage of Graphite Radioactive Waste

As noted earlier, the graphite radioactive waste generated during the operation of UGR was located in special reactor storage facilities or, in rare cases, in concrete containers and sent to storage facilities. As a rule, such storage facilities are located outside the reactor building (or facility), but within the sanitary protection zone. This is especially true for graphite radioactive waste storage facilities located at the sites of FSUE "MCC" (Zheleznogorsk, Krasnoyarsk region, Russia), FSUE "Mayak" Production Association (Ozersk, Chelyabinsk region, Russia), and JSC "PDC UGR."

To date, in the Russian Federation there are more than 30 types of radioactive waste storage, which can conditionally be divided into 3 main groups: in-depth insulated storage (trenches, bunkers, pits), in-depth open storage (storage reservoirs, holding pools, tailings), and separate buildings and structures [15]. The last two types of storage are less suitable for storing irradiated nuclear graphite. However there were isolated cases of temporary placement of graphite sleeves in this places [16]. In addition, in some reactor plants, there are special storage tanks (or receiving tanks) for graphite-containing sludge formed during the reconstruction of the reactor cells during its operation. However, most of the irradiated reactor graphite is located in structures that are placed in in-depth insulated structures.

Graphite radioactive waste storages made in the form of in-depth insulated structures can also be conditionally divided into three main types (this division is especially characteristic of irradiated graphite storages located in the Russian Federation):

(i) Trench type storages
(ii) Bunker (concrete) type storages
(iii) Storages located in rock mines

Trench type storages (Figure 1) are the most common type at the locations of the PUGR. They are usually used to isolate medium-active graphite radioactive waste (since the specific activity of ^{14}C varies in the range (10^4–10^6) Bq/g). Trench type storages were created with full burial in loamy soil (the mark of the top of the waterproofing coating almost coincides with the mark of natural soil). The compacted natural clay (20–30 cm thick) was used as the material of the side walls of such storages. Concrete containers (usually $1400 \times 1750 \times 850$ m in size and a wall thickness of ~500 mm) with irradiated graphite mixed with metal radioactive waste (aluminum channels, etc.) were placed in a pit 6 to 10 meters deep. The upper part of the trench type storage ("cover") was made of clay, loam, gravel, cement screed, concrete floor slabs, etc. The thickness of each layer is different and varies in the range from 0.5 cm to 100 cm.

Bunker (concrete) type storages are recessed near-surface reinforced concrete reservoirs with loading hatches and reinforced concrete plugs installed in them. The tank is divided by vertical partitions into compartments. A general view of such storage facilities is shown in Figure 2. A monolithic reinforced concrete slab with a thickness of 8 cm to 60 cm is located at the base of these objects. Coating waterproofing from oil bitumen and cement-sand screed with a thickness of 20 mm is applied to the slab. A layer of asphalt (3–10 cm thick), sprinkled with soil or sand (10–12 cm thick), is applied over the slab. Side walls are made of monolithic concrete with a thickness of 30–40 cm. Vertical waterproofing in the form of bitumen coating is applied to the outer edges of the walls of the tanks.

Access to such storages is difficult or impossible. Therefore, the temperature inside them can change only as a result of heat exchange with structural elements due to seasonal climate change, interaction with groundwater (if such cases occur), and/or the appearance of internal local heat sources.

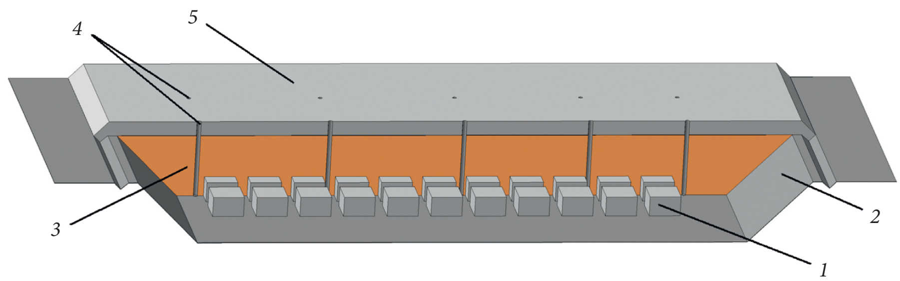

Figure 1: Appearance of the trench type storage: 1, containers with graphite waste; 2, compacted soil (clay); 3, clay-based safety barriers; 4, inspection tubes; 5, external protective screen ("cover").

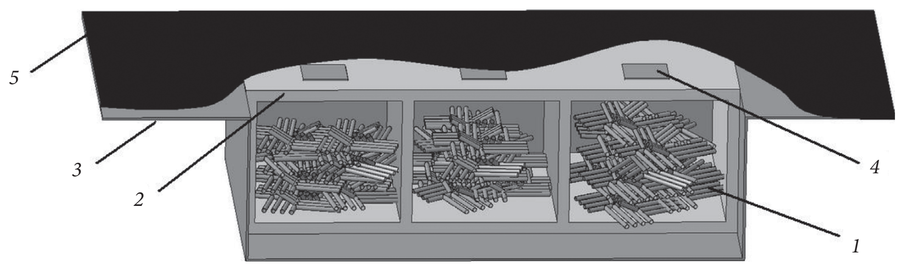

Figure 2: Appearance of the bunker (concrete) storage: 1, graphite radioactive waste; 2, reinforced concrete floors; 3, adjacent engineering structures; 4, reinforced concrete cork; 5, external screen (asphalt).

Storages located in rock mines (Figure 3) are less common.

These storages are reinforced concrete mine with a depth of more than 20 m. Irradiated graphite sleeves, fragments of graphite blocks and aluminum channels, ionization chambers, and thermocouple feed tubes are placed in bulk in the mine. The inner surface of the mine is lined with carbon steel with organic resin primer. The loading holes, which were concreted after the operation of the storage, are located in the upper ceiling of the mines. The volume of mines varies and ranges from 300 m^3 to 850 m^3. Part of the side wall of such storages is in direct contact with the rock massif. The other part is insulated with a layer of concrete up to 4 m thick. The qualitative and quantitative composition of the radioactive waste layers depend on the volume of work to remove them. In this case, the alternation of individual layers of graphite and pressed aluminum parts can be observed in storage.

Some storage facilities have fire detection and extinguishing systems. However, such systems are absent in most locations for irradiated graphite (especially those created in the middle of the last century).

Graphite refers to difficult to combustible materials; i.e., the possibility of its burning without additional supply of energy is excluded. The temperature of the onset of intense oxidation of graphite in air is $T = 450°C$ [17]. In this case, oxidation will be accompanied by the release of radionuclides ^{14}C, ^{36}Cl, etc. A more significant yield of radionuclides is possible only with ignition of graphite, which is possible only if there is sufficient air. The ignition temperature of graphite in air is 700–800°C. In the technical report [18], it is noted that, under certain conditions, mixed storage of graphite and other types of waste in bulk and in large volumes can lead to heat release. The analysis of heat release processes inside storages containing irradiated nuclear graphite is an important task in assessing and ensuring the safety of storage. This is due to the fact that the above-described storages are not designed for the storage of fuel radioactive waste, which mainly includes highly active vitrified waste.

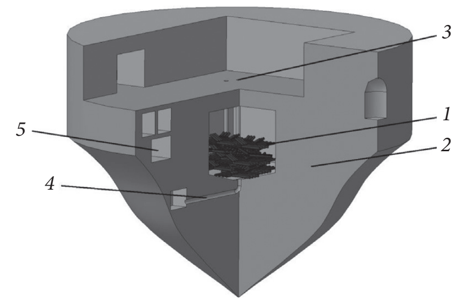

Figure 3: Appearance of storages located in rock mines: 1, graphite radioactive waste; 2, rock massif; 3, inspection system; 4, drainage system; 5, auxiliary rooms.

In this case, the accumulation of Wigner energy in graphite must be taken into account when analyzing heat release processes. Also, factors, conditions affecting the beginning of its isolation, and the possibility of their control should be taken into account. Determining the maximum values and dynamics of temperature changes during heating in the storage volume is also an important task.

3. Accumulation of Stored Energy in Irradiated Graphite

The amount of stored energy and the parameters of its release are determined by the conditions and duration of graphite irradiation in the reactor [19].

As described earlier in the course of the works [13, 20–22], irradiated graphite sleeves (Figure 4) were selected from uranium-graphite reactors and storage facilities. Selected graphite elements were sent for differential thermal analysis. The analysis results showed that the "worst-case" graphite sleeves (irradiated at the lowest possible temperature) of the cells of the flowing water-cooled UGR are the most critical from the point of view of the magnitude of the possible thermal effects due to the self-sustaining release of stored energy.

The characteristic release spectra of stored energy determined experimentally for graphite radioactive waste from storage facilities are shown in Figure 5.

The amount of stored energy in such graphite elements can reach 1250–1650 J/g. The temperature of the beginning of the release of stored energy for such elements is 90–100°C. These parameters are characteristic only of the upper sleeves of the control and protection system (CPS) cells. Their number is less than 10% of the total number of cells in the graphite stack of UGR with once-through coolant (reactor with an unclosed primary reactor coolant circuit). The main part of the cells has an irradiation temperature of the upper sleeves slightly higher than in the cells of CPS due to more intense volumetric energy release in graphite. The temperature of the beginning of the release of stored energy of such parts is estimated at the level of 120–130°C, and the amount of stored energy is 900–1200 J/g. The close Wigner energy release parameters for RBMKs are characteristic only for graphite displacers immersed in the channels of the CPS cells. The temperature of the cooling water in such cells is the lowest. It was previously determined [23, 24] that the temperature of graphite irradiation of displacer cells of the CPS of the RBMK reactor is 70–80°C, and the Wigner energy is 800–1000 J/g.

Wigner energy also accumulates in metal and metal-containing structures of the reactor. These include technological channels (including tensioning channels), thermocouples, metal plate flooring, tightening devices and bolted joints, fuel elements and their cladding, and control rods. For example, aluminum alloys used in Russian channel reactors, consisting of 96% highly pure aluminum (the remaining 4% are alloyed impurities Mn, Ti, Mg, and Fe), can accumulate up to 348 J/g of stored energy [25, 26]. Moreover, in copper-containing alloys it can accumulate up to 8 J/g of stored energy [27]. In addition, the value of the Wigner energy in irradiated metal carbides can be higher than in irradiated graphite. For example, in SiC its value reaches 2500 J/g [28]. Unfortunately, the issue of the content of stored energy and the conditions for its release in metal radioactive waste from reactors is not well understood.

4. Analysis of Factors Initiating the Release of Stored Energy

External influences on the landfill (or storage) of graphite radioactive waste and its contents include local or general temperature increase. As a result, the release of stored energy from irradiated graphite (to a lesser extent, from metal RW) can be initiated; chemical processes can be activated and catalyzed with the release of heat and gaseous reaction products that did not previously occur or proceeded extremely slowly. The consequences of such processes are difficult to predict. The main factors leading to the occurrence of such processes can be joined into the following groups:

(i) Natural (rise in groundwater level, earthquake, dramatic climate change, heavy rainfall)

(ii) Technogenic (short circuit in electrical systems, violation of storage operating modes, breakdown of the supporting equipment or equipment operating inside the facility, failure of the drainage system)

(iii) Anthropogenic (erroneous actions of personnel during maintenance or inspection of the storage facility, violation of fire safety rules, deliberate exposure or terrorist act)

The listed factors can affect the temperature increase inside the storage also when combined. For example, an increase in the level of groundwater, heavy rainfall, and failure of the drainage system can lead to a partial filling of the RW disposal facility with water. This, in turn, causes corrosion processes occurring with the release of heat. Also, a violation of its operation modes can lead to the appearance of liquid inside the storage.

In addition, factors leading to a sharp augmented waste heating can be a significant hazard. Factors that may occur during the liquidation and increase of the reliability of storage facilities are as follows:

(i) Ingress and ignition of flammable liquids (oil), etc.

(ii) Ingress of heated particles or fragments when using thermal cutting methods during the dismantling of storage structures

(iii) Supply of heated materials to the storage (pouring with concrete, creating safety barriers, etc.)

These factors increase the likelihood of initiating the Wigner energy release process and heating the contents of graphite RW storage. Figure 6 shows a principle (general) diagram of the start of heating of graphite RW in storage, irradiated in a once-through UGR at the lowest temperatures.

High humidity in the store due to the ingress of water into storage (especially groundwater containing various salts) can cause an increase in temperature inside this object due to the corrosive interaction of moisture and water solutions with aluminum structural elements located in it. Despite the fact that such RW is covered with a passivating

Figure 4: Fragments of sleeves removed from storage before and after core sampling.

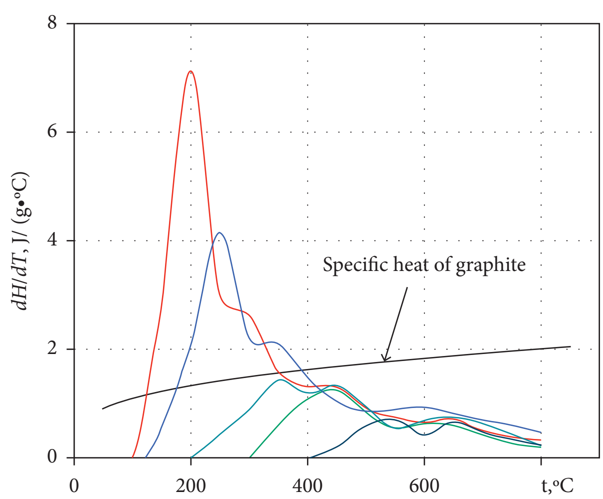

Figure 5: Spectra of the release of stored energy in irradiated graphite removed from storage facilities.

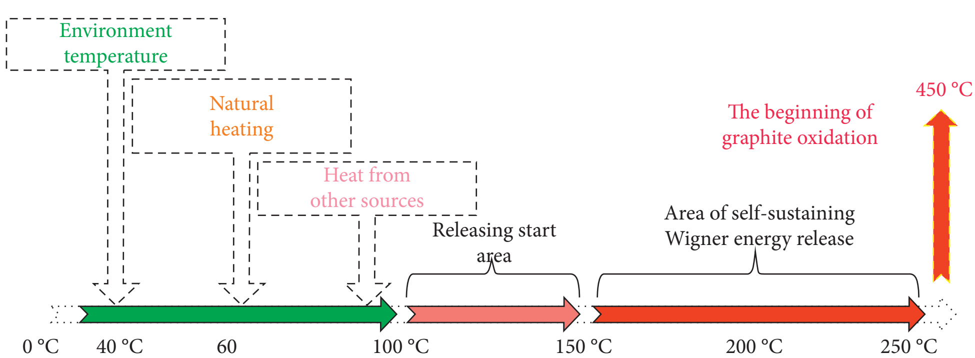

Figure 6: Schematic diagram of the start of heating of graphite radioactive waste in the storage.

film, consisting mainly of Al_2O_3, processes that cause corrosion can most likely occur. For example, an oxide film can be removed by interacting with some salts contained in the groundwater, or with an alkali solution. It is also possible mechanical removal due to mutual friction of parts when filling the storage and shrinkage of RW. It was shown in [29] that bacteria such as *Alternaria alternata* and *Pseudomonas aeruginosa* contribute to the destruction of the oxide film in particular and the corrosion of all aluminum parts in general.

Aluminum is a chemically active metal that intensively interacts with oxygen and water through reactions:

$$4Al + 3O_2 = 2Al_2O_3, \quad (1)$$

$$2Al + 6H_2O = 2Al(OH)_3 + 3H_2\uparrow. \quad (2)$$

Both reactions are exothermic. During the oxidation of aluminum by molecular oxygen (reaction (1)), Al_2O_3 is formed. In this case, the thermal effect of the chemical reaction is ≈ 1676 kJ. The interaction of aluminum with water occurs with the release of heat from 420 to 459.1 kJ (depending on the initial temperature of the water).

In addition, reaction (2) proceeds with the formation of gaseous hydrogen and describes the process of pitting corrosion. Local corrosion in form of spots, ulcers, or dots is the most common type of degradation of aluminum parts. Moreover, its speed depends on the concentration of chlorine ions, pH, and water temperature and averages 0.3–0.44 mm/year [30, 31]. The appearance of corroding aluminum parts is shown in Figure 7 [32].

In order to assess the corrosion rate caused by the possible ingress of groundwater into storage containing irradiated reactor graphite, a static experiment of long duration was carried out. The irradiated aluminum and iron-containing elements of the reactor located in the upper part of storage (the area in which contact with water was guaranteed to be excluded) were removed from the place of their location. One of the aluminum elements was sawed in the longitudinal direction to simulate damage and was placed in a transparent container with water taken from the drainage system of storage. Another element was also placed in the container without additional processing. It was found that the $NaHCO_3$ content in water did not exceed 7 mg/l, $MgSO_4$•$7H_2O$ 38 g/l, $CaCl_2$•$7H_2O$ 225 mg/l, and $MgCO_3$ 3 mg/l. Containers with irradiated aluminum and iron elements of the reactor were sealed and placed in one of the storage compartments. Thus, conditions were created as close as possible to the real conditions of their storage. It is worth noting that during the first (3–4) hours after the sawn aluminum element of the reactor was immersed inside the vessel with water, bubbles and condensation formed on the walls. The total duration of the experiment was 365 days. The appearance of irradiated metal parts after corrosion tests is shown in Figure 8.

Figure 8(a) shows that aluminum parts are more susceptible to pitting corrosion, complicated by the formation of organic films. The thickness of such films reached 2 mm. This confirms the assumption that bacteria make a significant contribution to the destruction of the passivating film and the surface of aluminum. The average corrosion rate determined by the weight and analytical method was ≈0.31 mm/year (calculated on the entire surface of the test element). According to Russian National State Standard 5272-90, aluminum in this case belongs to the low-resistance group of corrosion.

In contrast to the aluminum elements of the reactor extracted from storage, iron-containing parts are subject to uniform corrosion (Figure 8(b)). In addition, the tests revealed an intense separation of oxidized metal particles from the surface of the part. The corrosion rate measured by the volumetric analytical method was ≈0.5 mm/year.

In addition, galvanic corrosion may occur at the contact points between the irradiated reactor graphite and the aluminum structural elements of the UGR due to the occurrence of an uncompensated charge at the boundary of the region. The occurrence of such a process leads to corrosion cracking and the ingress of fluid into parts. The process is complicated by the formation of ions and electrons (mainly OH^-, H^+, e^-) due to the radiolysis of water in storage of graphite RW [33–35]. It is worth noting that the formation of aluminum carbides does not occur at a regulated temperature of storage operating. Such chemical reactions proceed only when graphite and aluminum (mainly in the form of powder) are heated to a temperature of 550°C [36]:

$$4Al + 3C = Al_4C_3, \quad (3)$$

$$Al_4C_3 + 12H_2O = 4Al(OH)_3 + 3CH_4\uparrow. \quad (4)$$

Reactions (3) and (4) are exothermic, in which 209 kJ and 1846 kJ are released, respectively. Most likely, the processes proceeding according to these reactions can not be the reason for the increase in a temperature of RW inside storage at the initial time and initiate the release of stored energy in irradiated graphite. However, they can intensify heating and heat distribution.

The results of analysis made above can be schematically presented as the dependence of the thermal effect of chemical reactions (as a measure of the risk of Wigner energy release) on factors that can cause heating of aluminum RW (Figure 9). It can be seen that the greatest amount of heat is released only during the stepwise heating due to the occurrence of reactions (3) and (2). This leads to an increase in a temperature of irradiated aluminum parts in storage, as well as RW in contact with them. In this case, Wigner energy is released in irradiated graphite, which catalyzes the occurrence of chemical reactions with the greatest thermal effect (reaction (4)).

It should be noted that the described factors are not exhaustive. The release of stored energy can be initiated from the top of storage (for example, by heating the air or getting a heated object into the storage). Report [18] shows other various causes of heat release (waste cementation, radioactive decay, microbiological interaction with organic waste, etc.). It is estimated that a temperature during heat generation associated with the monolithic treatment of waste during grouting can reach ≈60°C [37], while an elevated temperature can be observed for several days. By modeling, it is estimated that the temperature peak during heat release associated with radioactive decay can reach ≈60°C for 100 days and then slowly decline. It is noted that the temperature in this case will be higher in the center of the waste volume.

Thus, taking into account the presence of many factors, it is impossible to exclude the possibility that, in accordance with the principle diagram of the start of heating (Figure 6), they can, together or individually, cause the graphite heating to a temperature $T = 90$–100°C, which can lead to the release of stored energy, and when T150°C is reached, to a self-sustaining release of energy, accompanied by a sharper increase in temperature.

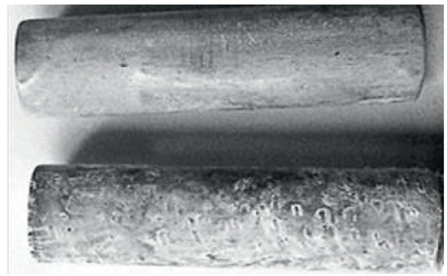

Figure 7: Appearance of corroding aluminum parts of UGR.

(a) (b)

Figure 8: Appearance of aluminum (a) and iron-containing (b) elements of the reactor after corrosion tests (365 days).

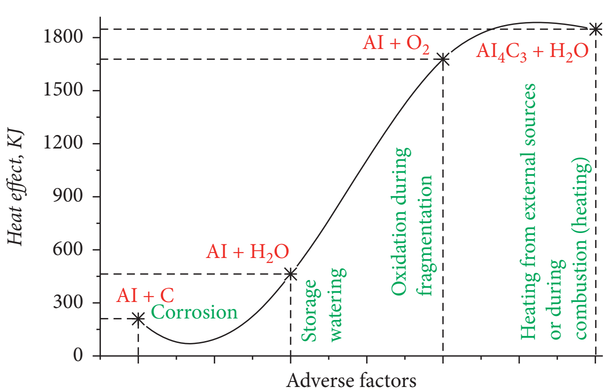

Figure 9: Dependence of the thermal effect of chemical reactions on factors capable of initiating them.

Moreover, taking into account the effect of energy dissipation (with jumbled parts), the greatest thermal effects should be expected in the case of local heating in sufficiently massive layers of graphite in storage.

5. Modeling the Release of Stored Energy in the Irradiated Graphite-Aluminum System

In the course of model studies, a calculation analysis of possible thermal effects and dynamics of changes in temperature fields during the release of stored energy in graphite parts located in concrete type storages and storages located in rock mines was carried out.

In order to determine the maximum possible thermal effects due to the release of Wigner energy, the most unfavorable situation is considered. Namely, it is assumed that in the local area of storage there is an accumulation of graphite parts irradiated in the reactor at the lowest temperature and having the most significant (from the point of view of possible thermal effects) parameters of the release of stored energy (Figure 5, the red curve).

These parameters correspond to graphite RW in the form of replaceable elements irradiated for a regular period in the reactor at low temperatures and containing the maximum possible amount of stored energy ("worst-case" graphite). The total amount of stored energy in this case is 1250–1650 J/g.

Temperature fields were calculated by solving the one-dimensional nonstationary heat conduction problem. The computational domain diagram is shown in Figure 10. The layer of irradiated graphite elements of thickness L_{gr} is in contact with the layer of irradiated aluminum elements of thickness L_{al} at the point C. In this case, horizontal planes passing through the points A and D are the boundaries of the area beyond which concrete or air is located. Such conditions were chosen with the aim of analyzing the temperature fields for various placement of graphite RW inside storage. A conservative case was also considered in which irradiated

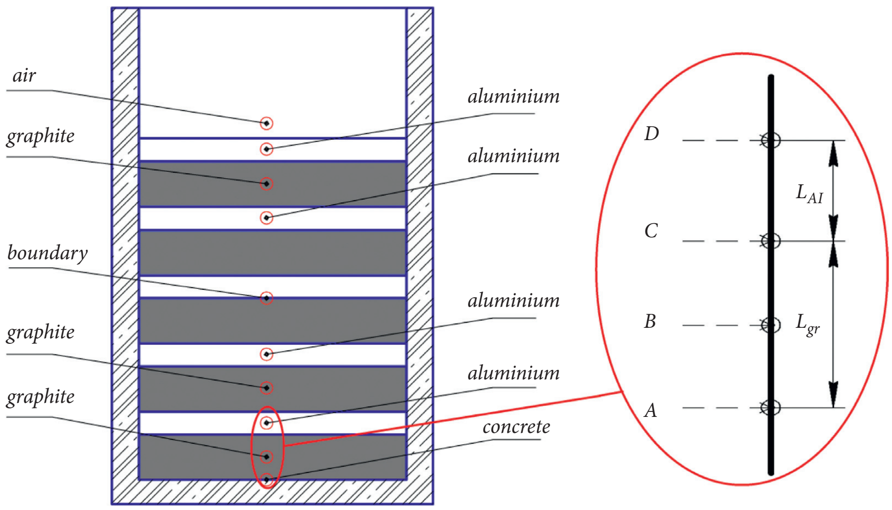

Figure 10: Computational domain diagram.

graphite and aluminum are in adiabatic conditions. The horizontal plane passing through the point B is the central plane of the layer of irradiated graphite elements.

In addition, the calculations took into account that the supply of heat in an amount sufficient to initiate the process of releasing the stored energy can be carried out in various sections of the considered system (A, B, C, D). The task was solved for the following cases:

(1) *Heating in a Horizontal Plane Passing through the Point A.* A situation is simulated when heat is supplied to the surface of irradiated graphite, for example, when the concrete base of the graphite RW storage is heated to a temperature exceeding the temperature of the self-sustaining release of stored energy ($T > 100^{\circ}C$) for graphite operated at the lowest temperatures. Heating of the concrete base of the storage facility with irradiated reactor graphite is possible in case of violation of the passive cooling mode (for example, for storage facilities located in the mine workings of a rock mass, or during deep disposal of radioactive waste). Also, such heating is possible in the event of a fire in adjacent rooms (with a compact arrangement of objects).

(2) *Heating in a Horizontal Plane Passing through the Point B.* A situation is simulated when heat is generated inside irradiated graphite, for example, due to the occurrence of nuclear or other reactions (for the case of a mixture of graphite and fuel fragments), as a result of ingress of combustible materials into storage or heat transfer from other more heated elements. This situation occurs when flammable materials are placed in a storage facility (for example, radiation-contaminated rags, paper, cloth, etc.). This plane also maintains a temperature exceeding the temperature of the self-sustaining release of stored energy ($T > 100^{\circ}C$).

(3) *Heating in a Horizontal Plane Passing through the Point C.* A situation is simulated when heat is released at the point of contact of graphite with aluminum, for example, due to the occurrence of exothermic reactions during galvanic corrosion of the latter. This situation is most typical for storage facilities that are at risk of being flooded by groundwater or water circulating in the rock mass. The boundary conditions are similar to the boundary conditions when graphite is heated at the points A and B.

(4) *Heating in a Horizontal Plane Passing through the Point D.* A situation is simulated when heat is released on the surface of a layer of irradiated aluminum elements, for example, when air is heated or a hot object gets in, and also due to exothermic reactions during pitting corrosion. Here the situation is simulated when the heating of aluminum occurs during fragmentation works using thermal cutting methods or in violation of the heat removal mode. At this point, the temperature is also above 100°C.

It is worth noting that the temperature of graphite, aluminum, air, and concrete at the initial time is taken equal to 20°C. The methodology for calculating temperature fields, the mathematical model, the initial data, and also the parameters for the release of stored energy are presented in [13, 20–22]. The thickness of the layer of graphite RW L_{gr} and irradiated aluminum parts L_{al} was calculated based on the geometrical dimensions of storage (it was believed that its cross-sectional area does not change in height), irradiated graphite sleeves, and fragmented aluminum channels. The number of the latter was estimated by averaging the volume of radioactive waste generated during their extraction from the UGR. Thus, the values of L_{gr} and L_{al} in the calculations were taken equal to 2 m and 0.5 m, respectively. The results of calculating the temperature fields during heating at the points A and B are presented in Figure 11.

Figure 11(a) shows that when the surface of irradiated graphite is heated at the point A from the side of the heat insulator and concrete, the temperature of the graphite layer

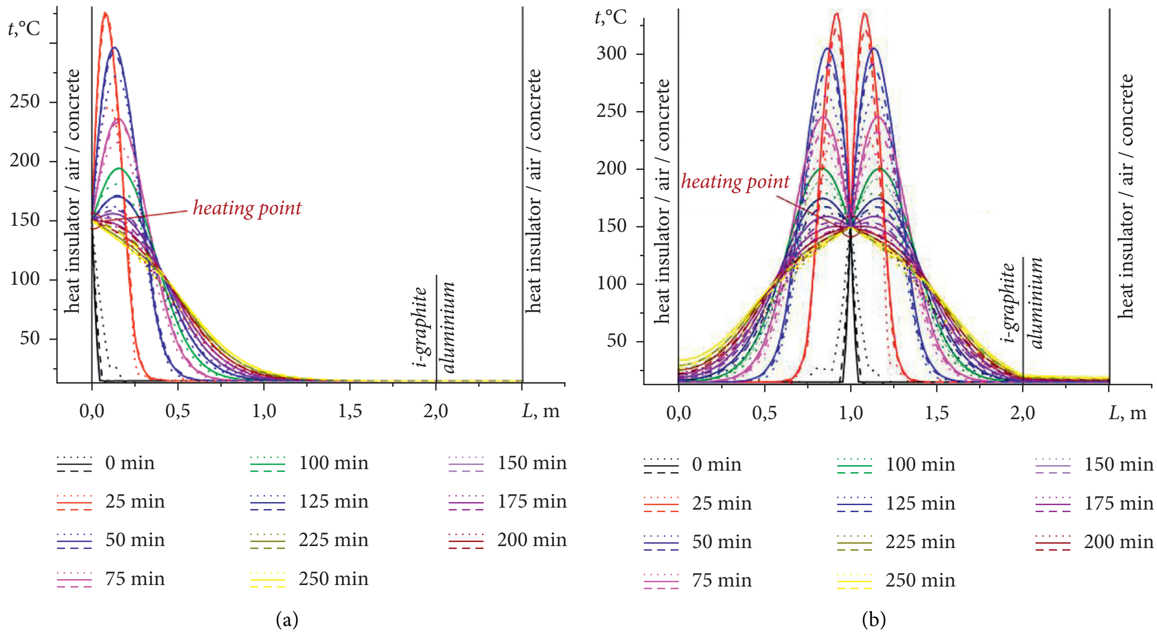

Figure 11: Dynamics of temperature fields in the irradiated graphite-aluminum system during heating in planes A (a) and B (b). Solid line: a heat insulator located on the border of the region (adiabatic conditions); broken line: concrete located on the border of the region; dotted line: air at the border of the region.

increases up to 325°C during the first 25 minutes. Subsequently, the surface temperature decreases, and heat propagates along the layer to the right boundary of the computational domain, passing through aluminum. It also shows that, within 250 minutes (the time during which a temperature in the surface layer of graphite decreases to a temperature of the heater), the front of the heat wave slows down to a depth of 1.5 meters from the surface of graphite. Thermodynamic equilibrium, at which a temperature at all points of the region under consideration will be equal to 150°C, is possible only under adiabatic conditions. Otherwise, the released heat is dissipated and transferred to the environment. It is a peculiarity of RW located in the air (dotted line in Figure 11(a)). Despite the fact that, in the regions of graphite closer to the heating surface, the fraction of the released stored energy is higher, the process of its release is more intense (thermal effects are more expressed in dynamics and amplitude). Intense heat dissipation occurs. This, in turn, leads to a decrease in the intensity of Wigner energy release and makes it impossible to further anneal crystal lattice imperfections and, accordingly, increase a temperature (without additional energy supply).

When irradiated graphite is heated in the plane B (Figure 11(b)), a uniform and almost symmetrical movement of the heat wave front to the layer surface and the contact area with aluminum occurs. With this formulation of the task, the dynamics of temperature fields is similar to the dynamics described above. However, heat is removed more intensively through the upper boundary of the computational domain (i.e., through the aluminum layer). At the lower boundary in 250 minutes the temperature reaches 27°C. Its further growth will be accompanied by the beginning of the release of stored energy. In this case, a change in the direction of the temperature gradient will occur, but it does not significantly change the thermal balance of the system. It is worth noting that a temperature at the left boundary does not reach a temperature of phase transitions and the release of stored energy in irradiated aluminum.

In the case of heat supply from the aluminum layer, the dynamics of the temperature fields changes (Figure 12).

When irradiated graphite is heated in the contact area with an aluminum layer (plane C), the stored energy is released in irradiated graphite (Figure 12(a)). In this case, the regularities of temperature field change inside a graphite layer are similar, as during heating at the points A and B. However, it is seen that part of the heat is transferred to the aluminum layer, as a result of which the layer is heated to a temperature of not more than 150°C. The heating rate, to a greater extent, depends not on the intensity of the release of stored energy, but on the conditions at the upper boundary of the computational domain, i.e., on the efficiency of the heat removal.

In the case of heat supply at the point D, the aluminum layer is first heated and then the layer of irradiated graphite elements. However, at an initial heating temperature of 150°C, the energy dissipates in graphite and in the environment. Figure 12(b) shows that the supplied energy is insufficient to initiate self-sustaining release of stored energy. In this case, heating of irradiated graphite due to this process is possible. This is evidenced by a small peak (50 minutes after the start of heat supply) when graphite was heated under adiabatic conditions and when it came into contact with the concrete walls of the storage. However, the temperature increment in this case does not exceed 1–3°C.

The time dependences of the temperature change of irradiated nuclear graphite and aluminum at the reference

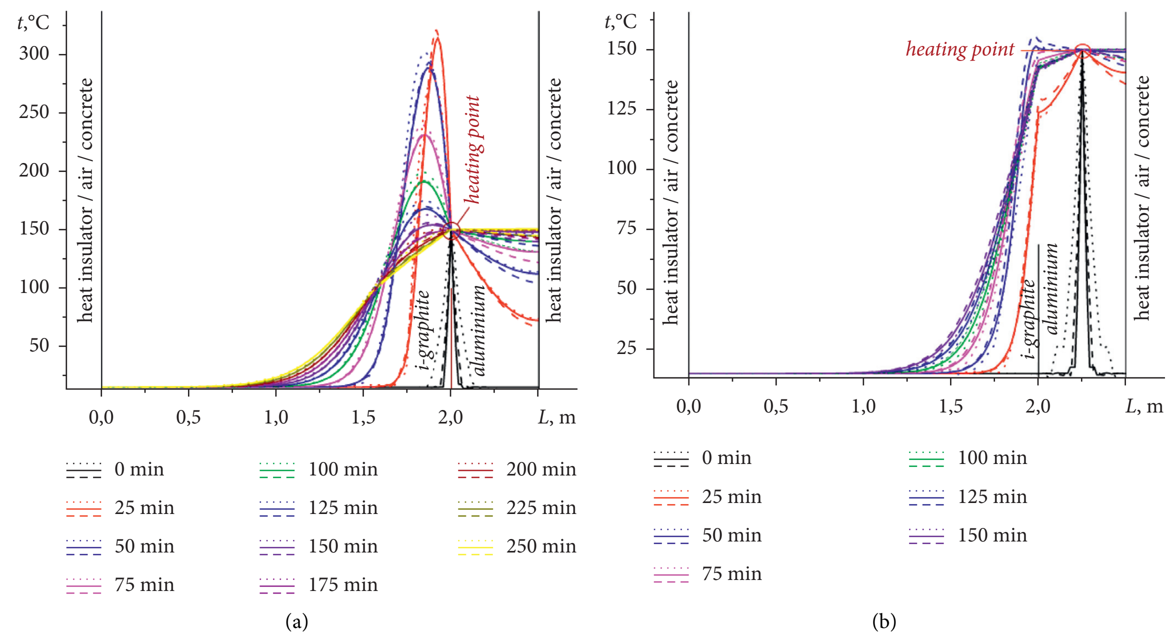

FIGURE 12: Dynamics of temperature fields in the irradiated graphite-aluminum system during heating in planes C (a) and D (b). Solid line: a heat insulator is located on the border of the region (adiabatic conditions); broken line: concrete is located on the border of the region; dotted line: there is air at the border of the region.

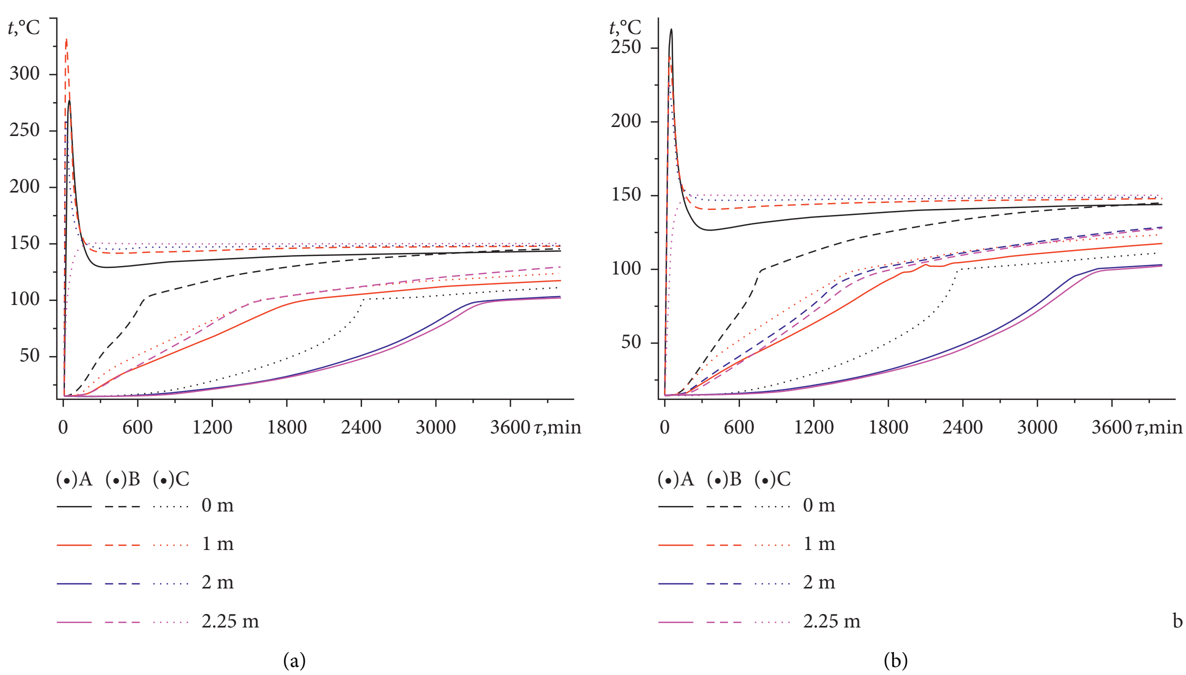

FIGURE 13: Continued.

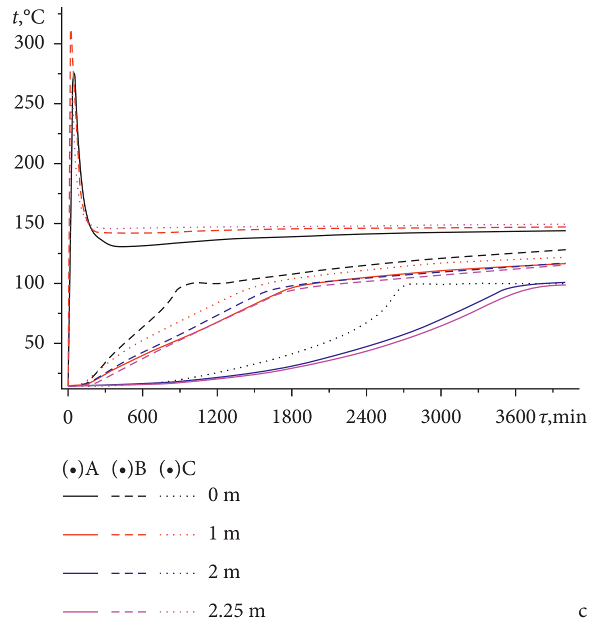

(c)

Figure 13: Time dependences of temperature changes at various points lying on the axis of a graphite and aluminum under various boundary conditions. (a) A heat insulator is located at the boundary of the region (adiabatic conditions). (b) There is air at the border of the region. (c) There is concrete on the border of the region.

points at a distance of 0, 1, 2, and 2.25 m from the lower boundary are also calculated (Figure 13). Heat is supplied in the planes A, B, and C in each individual case.

Figure 13 shows that the most critical region in terms of the intensity of the release of stored energy is the heat supply region. With an increase in the linear dimensions of the graphite layer, there occurs an increase in the proportion of energy spent on its heating, and not on the initiation of the process of releasing stored energy. On the other hand, under conditions of complete or partial absence of heat exchange with the environment (Figures 13(a) and 13(c)), the greatest temperature increase at the initial moment of time (the first 30 minutes) is observed when heat is supplied to the geometric center of the graphite layer. To a lesser extent, such effects occur under conditions of heat removal, for example, into the environment (Figure 13(b)).

6. Conclusion

Based on the results of the study, the following conclusions can be drawn:

(1) Taking into account the presence of many factors, it is impossible to exclude the possibility that they can, together or separately, cause the heating of graphite to a temperature of $T = 90–100°C$, which leads to the beginning of the release of stored energy in graphite fragments with the most critical parameters of its release, and upon reaching $T\,150°C$ to self-sustaining energy release, accompanied by a sharper increase in temperature.

(2) In contrast to the fuel highly active RW in graphite RW heating is local and short-term. The duration of the most intensive stage of the process is not more than 100 minutes.

(3) As a result of modeling the process of Wigner energy release in irradiated graphite and aluminum located in various types of storages, it was determined that the dynamics of temperature fields and the temperature value in different areas of the storages depend on the place of heat supply (the reason that caused local heating), as well as on the conditions at the boundary of the area (i.e., the location of the considered RW inside the storage). It is shown that the greatest amplitudes thermal effects have are when the stored energy is released in graphite RW located near the concrete walls of the storage facility, as well as in direct contact with irradiated aluminum RW. In these cases, a local temperature can reach more than 300°C (for adiabatic conditions 375°C), which does not lead to the initiation of the process of release of nuclides from graphite RW and the beginning of the release of Wigner energy in irradiated aluminum.

(4) Considering the fact that the storages contain graphite elements irradiated in the reactor over a wide range of temperatures and neutron fluxes, it should be noted that self-sustaining release of stored energy is possible only for an insignificant part (<10%). Taking into account the peculiarities of filling storages, even in the case of layer-by-layer filling with graphite and aluminum RW, graphite

elements in the layers of graphite RW are most likely to be distributed randomly. The heat dissipation factor in the case of the release of stored energy significantly reduces the parameters of thermal effects, compared with the parameters obtained in this article.

Data Availability

The article contains previously unpublished data.

Conflicts of Interest

The authors declare that they have no conflicts of interest.

Acknowledgments

This work was supported by the Tomsk Polytechnic University Competitiveness Enhancement Program.

References

[1] IAEA, *Progress in Radioactive Graphite Waste Management, No. IAEA-TEDDOC-1647*, International Atomic Energy Agency, Vienna, Austria, 2010, https://www-pub.iaea.org/MTCD/Publications/PDF/te_1647_web.pdf.

[2] A. N. Dorofeev, E. A. Komarov, E. V. Zaharova et al., "On reactor graphite disposal," *Radioactive Waste*, vol. 2, no. 7, pp. 18–30, 2019, in Russian.

[3] Evolution of the Context of Irradiated Graphite Management in France–Impacts on R&D, Technical Meeting on the International Project on Irradiated Graphite Processing Approaches, 6th–9th of June, 2017.

[4] G. Holt, *Radioactive Graphite Management at UK Magnox Nuclear Power Stations*, International Atomic Energy Agency, Vienna, Austria, 2017, https://www-pub.iaea.org/MTCD/publications/PDF/ngwm-cd/PDF-Files/paper_17_(Holt).pdf.

[5] Environment Agency, *Wigner Energy in Irradiated Graphite and post-closure Safety, Technical Report*, https://assets.publishing.service.gov.uk/government/uploads/system/uploads/attachment_data/file/290413/sp3-080-tr-e-e.pdf, Environment Agency No. P3–80/TR, Bristol, UK, 2002, https://assets.publishing.service.gov.uk/government/uploads/system/uploads/attachment_data/file/290413/sp3-080-tr-e-e.pdf.

[6] IAEA, *Processing of Irradiated Graphite to Meet Acceptance Criteria for Waste Disposal, Results of a Coordinated Research Project, No. 1790*, International Atomic Energy Agency, Vienna, Austria, 2015, https://www-pub.iaea.org/books/IAEABooks/10978/Processing-of-Irradiated-Graphite-to-Meet-Acceptance-Criteria-for-Waste-Disposal.

[7] P. Minshall and A. Jones, "Modeling the release of wigner energy during irradiated graphite disposal: are we doing it right?" in *Proceedings of the International Nuclear Graphite Specialists' Meeting INGSM-20*, Bruges, Belgium, September 2019.

[8] J. C. Bell, H. Bridge, A. H. Cottrell, G. B. Greenough, W. N. Reynolds, and J. H. W. Simmons, "Stored energy in the graphite of power-production reactors," *Philosophical Transactions of the Royal Society A*, vol. 1043, no. 254, pp. 361–395, 1962.

[9] P. C. Minshall and A. J. Wickham, *The Description of Wigner Energy and its Release from Windscale Pile Graphite for Application to Waste Packaging and Disposal*, Report IAEA-NGWM/CD-01, IAEA, Vienna, Austria, 2001, http://www.iaea.org/inis/collection/NCLCollectionStore/_Public/32/039/32039324.pdf?r=1.

[10] B. T. Kelly, "Radiation damage in graphite and its relevance to reactor design," *Progress in Nuclear Energy*, vol. 2, no. 4, pp. 219–269, 1978.

[11] C. D. Latham, M. I. Heggie, M. Alatalo, S. Oberg, and P. R. Briddon, "The contribution made by lattice vacancies to the Wigner effect in radiation-damaged graphite," *Journal of Physics. Condensed Matter: An Institute of Physics Journal*, vol. 25, pp. 135403–135413, 2013.

[12] A. Chartier, L. van Brutzel, and J. Pageot, "Irradiation damage in nuclear graphite at the atomic scale," *Carbon*, vol. 133, pp. 224–231, 2018.

[13] A. O. Pavliuk, S. G. Kotlyarevskiy, and E. V. Bespala, "Analysis of Winger energy release process in graphite stack of shutdown uranium-graphite reactor," *IOP Conference Series: Materials Science and Engineering*, vol. 93, pp. 1–5, 2015.

[14] A. Wickham, H.-J. Steinmetz, P. O'Sullivan, and M. I. Ojovan, "Updating irradiated graphite disposal: project 'GRAPA' and the international decommissioning network," *Journal of Environmental Radioactivity*, vol. 171, pp. 34–40, 2017.

[15] V. S. Gupalo, "Technological issues to enhance the safety of historic radioactive waste repositories," *Mountain Information and Analytical Bulletin*, vol. 9, pp. 112–116, 2009, in Russian.

[16] A. M. Izmestiev, A. O. Pavliuk, and S. G. Kotlyarevskiy, "The experience of JSC "DNRC" in solving the problem of RW of non-project storage facilities," *Safety of nuclear technology and the environment*, vol. 3, no. 4, pp. 84–87, 2013, in Russian.

[17] E. V. Bespala, A. O. Pavlyuk, S. G. Kotlyarevskii, I. Y. Novoselov, and Y. R. Bespala, "Heat treatment of irradiated graphite in an oxidizing atmosphere," *Solid Fuel Chemistry*, vol. 52, no. 5, pp. 328–335, 2018.

[18] EPRI, *Graphite Decommissioning: Options for Graphite Treatment, Recycling or Disposal, Including a Discussion of Safety-Related Issues, Technical Report No. 1013091*, EPRI, Washington, DC, USA, 2006, http://www.ngnpalliance.org/index.php/resources/download/czo0NDoiL2ltYWdlcy9nZW5lcmFsX2ZpbGVzLzAwMDAwMDAwMDAwMTAxMzA5MS5QREYiOw.

[19] T. Iwata, "Fine structure of Wigner energy release spectrum in neutron irradiated graphite," *Journal of Nuclear Materials*, vol. 133-134, pp. 361–364, 1985.

[20] A. A. Tsyganov, S. G. Kotlyarevskiy, A. O. Pavliuk, I. V. Shamanin, and V. N. Nesterov, "Storage energy in graphite of shutdown production uranium-graphite reactors," *Bulletin of the Tomsk Polytechnic University*, vol. 312, pp. 32–38, 2008.

[21] A. I. Dostov, "A method of calculating the rate of release of Wigner energy in heat conduction problems for irradiated graphite," *High Temperature*, vol. 43, no. 2, pp. 259–265, 2005.

[22] A. O. Pavliuk, S. G. Kotlyarevsky, E. V. Bespala, and I. Y. Novoselov, "Dynamics of temperature fields during Wigner energy release in bulk graphite irradiated at low temperature," *Journal of Nuclear Materials*, vol. 515, pp. 303–311, 2019.

[23] A. I. Dostov, "Wigner energy in the plungers in the safety and control system of RBMK reactors," *Voprosy Atomnoi Nauki i*

Tekhniki, Seria Fizika Yadernykh Reaktorov, vol. 3, pp. 22–31, 2001, in Russian.

[24] P. A. Platonov, E. V. Burlakov, O. K. Chugunov, A. I. Dostov, V. M. Alekseev, and E. I. Smorodkin, "Computational-experimental investigation of the Wigner energy and the physical properties of plunger graphite in the safety and control system of an RBMK reactor," *Atomic Energy*, vol. 94, no. 4, pp. 225–237, 2003.

[25] A. V. Mostovshchikov, A. P. Ilyin, and M. A. Zakharova, "Energy storage in aluminum nanopowder in stress-strain state of crystal lattice," *Bulletin of the Tomsk Polytechnic University. Geo Assets Engineering*, vol. 327, pp. 77–82, 2016.

[26] A. V. Mostovshchikov, A. P. Ilyin, A. A. Azanov, and I. S. Egorov, "The energy stored in the aluminum nanopowder irradiated by electron beam," *Key Engineering Materials*, vol. 685, pp. 639–642, 2016.

[27] A. W. Overhauser, "Stored energy measurements in irradiated copper," *Physical Review*, vol. 94, no. 6, pp. 1551–1557, 1954.

[28] L. L. Shead, Y. Katoh, T. Koyanagi, and K. Terrani, "Stored energy release in neutron irradiated silicon carbide," *Journal of Nuclear Materials*, vol. 514, pp. 181–188, 2019.

[29] D. V. Belov, T. N. Sokolova, and V. P. Kartashov, "Corrosion of aluminum and aluminum alloys under the influence of microorganisms," *Chemistry and chemical technology*, vol. 50, pp. 60-61, 2007, in Russian.

[30] H. Godfrey, M. Hayes, D. Anderson, S. Rawlinson, J. Borwick, and J. Clifford, "Corrosion of 1050, 1085, and 5083 grade aluminium in the pore water of a GGBS/CEM I grout up to 777 d," *Journal of Nuclear Materials*, vol. 515, pp. 257–266, 2019.

[31] Y. S. Kim, G. L. Hofman, A. B. Robinson, J. L. Snelgrove, and N. Hanan, "Oxidation of aluminum alloy cladding for research and test reactor fuel," *Journal of Nuclear Materials*, vol. 378, no. 2, pp. 220–228, 2008.

[32] V. A. Zuev, R. A. Rud, M. V. Tretiyakov, Y. A. Kushtym, and V. S. Krasnorutskiy, "Contact corrosion of aluminum and its alloys in the aquatic environment," *Nuclear and radiation safety*, vol. 3, no. 67, pp. 24–30, 2015, in Russian.

[33] P. Scott, "A review of irradiation assisted stress corrosion cracking," *Journal of Nuclear Materials*, vol. 211, no. 2, pp. 101–122, 1994.

[34] IAEA, *Corrosion of Research Reactor Aluminium Clad Spent Fuel in Water, IAEA-TECDOC-1637*, International Atomic Energy Agency, Vienna, Austria, 2003, https://www-pub.iaea.org/MTCD/Publications/PDF/te_1637_web.pdf.

[35] V. Čuba, V. Múčka, and M. Pospišil, "Radiation induced corrosionof nuclear fuel and materials" *Advances in Nuclear Fuel*, S. T. Revankar, Ed., pp. 27–52, Intech Open, London, UK, 2012, http://www.intechopen.com/books/advances-in-nuclear-fuel/radiation-induced-corropen-of-nuclear-fuel-and-materials.

[36] T. Carlsson, P. Kotiluoto, O. Vilkamo, T. Kekki, I. Auterinen, and K. Rasilainen, *Chemical Aspects on the Final Disposal of Irradiated Graphite and Aluminium*, VTT Technology, Otaniemi, Finland, 2014.

[37] R. M. Guppy, J. McCarthy, and S. J. Wisbey, "Technical assessment of the significance of Wigner energy for disposal of graphite wastes from the Windscale Piles," in *Proceedings of the IAEA Technical Committee Meeting on Characterisation, Treatment and Conditioning of Radioactive Graphite from Decommissioning of Nuclear Power Reactors*, pp. 1–18, Manchester, UK, 1999.